*J Cell Sci*. Author manuscript; available in PMC 2016 July 26.

Published in final edited form as:

*J Cell Sci*. 2013 September 15; 126(Pt 18): 4187–4194. doi:10.1242/jcs.127571.

# Fibrillin-1 directly regulates osteoclast formation and function by a dual mechanism

**Kerstin Tiedemann**[1,2], **Iris Boraschi-Diaz**[1,2], **Irina Rajakumar**[1,*], **Jasvir Kaur**[3], **Peter Roughley**[2], **Dieter P. Reinhardt**[1,3,‡], and **Svetlana V. Komarova**[1,2,3,‡,§]

[1]Faculty of Dentistry, McGill University, 3640 rue University, Montreal, Quebec, Canada, H3A 0C7

[2]Shriners Hospital for Children – Canada, 1529 Cedar Ave, Montreal, Quebec, Canada, H3G 1A6

[3]Department of Anatomy and Cell Biology, Faculty of Medicine, McGill University, 3640 rue University, Montreal, Quebec, Canada, H3A 0C7

## Summary

Mutations in the fibrillin-1 gene give rise to a number of heritable disorders, which are all characterized by various malformations of bone as well as manifestations in other tissues. However, the role of fibrillin-1 in the development and homeostasis of bone is not well understood. Here, we examined the role of fibrillin-1 in regulating osteoclast differentiation from primary bone-marrow-derived precursors and monocytic RAW 264.7 cells. The soluble N-terminal half of fibrillin-1 (rFBN1-N) strongly inhibited osteoclastogenesis, whereas the C-terminal half (rFBN1-C) did not. By contrast, when rFBN1-N was immobilized on calcium phosphate, it did not affect osteoclastogenesis but modulated osteoclast resorptive activity, which was evident by a larger number of smaller resorption pits. Using a panel of recombinant sub-fragments spanning rFBN1-N, we localized an osteoclast inhibitory activity to the 63 kDa subfragment rF23 comprising the N-terminal region of fibrillin-1. Osteoclastic resorption led to the generation of small fibrillin-1 fragments that were similar to those identified in human vertebral bone extracts. rF23, but not rFBN1-N, was found to inhibit the expression of cathepsin K, matrix metalloproteinase 9 and Dcstamp in differentiating osteoclasts. rFBN1-N, but not rF23, exhibited interaction with RANKL. Excess RANKL rescued the inhibition of osteoclastogenesis by rFBN1-N. By contrast, rF23 disrupted RANKL-induced $Ca^{2+}$ signaling and activation of transcription factor NFATc1. These studies highlight a direct dual inhibitory role of N-terminal fibrillin-1 fragments in osteoclastogenesis, the sequestration of RANKL and the inhibition of NFATc1 signaling, demonstrating that osteoclastic degradation of fibrillin-1 provides a potent negative feedback that limits osteoclast formation and function.

[§]Author for correspondence (svetlana.komarova@mcgill.ca).
[*]Present address: London Health Science Center, London, ON, Canada
[‡]These authors contributed equally to this work

**Author contributions**

K.T., D.P.R. and S.V.K. designed the experiments, interpreted the results and prepared the manuscript. K.T. performed the experiments. I.B.D. contributed to experimental design and performed the experiments. I.R. performed key preliminary experiments. J.K. prepared recombinant fibrillin fragments. P.R. provided human bone samples. All authors read and approved the manuscript.

Supplementary material available online at http://jcs.biologists.org/lookup/suppl/doi:10.1242/jcs.127571/-/DC1

**Keywords**

Calcium signaling; Fibrillin; NFATc1; Osteoclastogenesis; RANKL

## Introduction

Mutations in the fibrillin-1 gene cause a range of connective tissue disorders characterized by variable clinical symptoms in the skeletal, cardiovascular and ocular systems. These disorders are termed type I fibrillinopathies and include, among others, Marfan syndrome (MFS), dominant Weill-Marchesani syndrome, geleophysic dysplasia and acromicric dysplasia (Hubmacher and Reinhardt, 2011). The skeletal symptoms in these disorders show a remarkable range, from long bone overgrowth, arachnodactyly and loose joints in MFS to short stature and brachydactyly in the other type I fibrillinopathies, suggesting that fibrillin-1 plays a major role in regulating skeletal homeostasis. Osteopenia is a hallmark of MFS and may be present in Weill–Marchesani syndrome (Giordano et al., 1997; Pyeritz, 2000).

This study is motivated by a largely unexplained low bone mass present particularly in individuals with MFS that likely increases the risk of fractures as the patient age increases due to successful treatment of cardiovascular aneurysms (Kohlmeier et al., 1995). Children with MFS have significantly lower bone mineral density compared with healthy height-matched controls (Kohlmeier et al., 1995; Moura et al., 2006), which was shown to persist in both women (Kohlmeier et al., 1995; Le Parc et al., 1999) and men (Carter et al., 2000; Le Parc et al., 1999) with MFS. While no appropriately powered study was performed yet on the fracture risk in older MFS patients, studies with small numbers of young patients indicate increased peripheral traumatic fractures (Grahame and Pyeritz, 1995; Kohlmeier et al., 1995).

The fibrillin super-family of large cysteine-rich glycoproteins consists of fibrillin-1, -2 and -3 and the latent transforming growth factor (TGF) β-binding proteins (LTBPs). Fibrillins constitute the backbone of extracellular microfibrils, which confer structural and functional integrity to all tissues including the skeleton (Hubmacher et al., 2006; Ramirez et al., 2007). In the skeletal system, the fibrillins are expressed in long bones, ribs, vertebral bodies and cartilage (Arteaga-Solis et al., 2001; Keene et al., 1991; Kitahama et al., 2000; Quondamatteo et al., 2002; Sabatier et al., 2011; Zhang et al., 1995). Fibrillins and fibrillin-containing microfibrils regulate the bioavailability of growth factors of the TGFβ superfamily including TGFβ and bone morphogenetic proteins (BMPs) (Neptune et al., 2003; Nistala et al., 2010b; Sengle et al., 2008). In turn, TGFβ and BMPs are important regulators of bone growth and remodeling (Giannoudis et al., 2007; Guo et al., 2008; Janssens et al., 2005; Quinn et al., 2001). Elevated TGFβ levels are a major disease-causing factor in MFS and other fibrillinopathies (Doyle et al., 2012; Le Goff and Cormier-Daire, 2012).

Changes in bone are regulated by the activities of osteoblasts, the cells responsible for new bone formation, and osteoclasts that remove mineralized tissue. In mouse models of progressively severe MFS, *Fbn1*$^{mgR/mgR}$ (Nistala et al., 2010a), as well as *Fbn1*$^{-/-}$ (Nistala et al., 2010c), osteoclastogenesis was reported to increase in a TGFβ- and osteoblast-

dependent manner. Importantly, in the *Fbn1*$^{mgR/mgR}$ mice, treatment with alendronate, a bisphosphonate that directly targets osteoclasts, but not with an angiotensin receptor I antagonist that lowers TGFβ signaling, resulted in significant improvement of bone quality (Nistala et al., 2010a). These data suggest that osteoclasts are critical, but unexplored, players in the skeletal pathophysiology of MFS and possibly other type I fibrillinopathies. In this study, we addressed the direct role of fibrillin-1 in regulating osteoclast differentiation and function.

## Results

### Fibrillin-1 and fibrillin-2 are produced and secreted by differentiating osteoblasts

First we demonstrated that fibrillin-1 and fibrillin-2 are expressed and secreted by differentiating osteoblasts (supplementary material Fig. S1). Both, *Fbn1* and *Fbn2* mRNA were strongly induced during the first week of osteoblast differentiation, and the development of fibrillin-1-containing microfibrils was apparent by immunofluorescence during the first week of differentiation. Fibrillin-1 was undetectable in cells of osteoclast lineage (supplementary material Fig. S1D).

### Fibrillin-1 affects function and differentiation of osteoclasts

Since full-length fibrillin-1 is not amenable for sufficient recombinant production due to its propensity to aggregate (Lin et al., 2002), we utilized recombinant N-terminal (rFBN1-N) and C-terminal (rFBN1-C) halves of fibrillin-1 (Jensen et al., 2001). rFBN1-N and rFBN1-C were immobilized on calcium phosphate, and osteoclast differentiation from bone marrow cells was induced with MCSF (50 ng/ml) and RANKL (50 ng/ml). The presence of fibrillin-1 on calcium phosphate did not affect osteoclast formation (Fig. 1A top, B). Although the total area resorbed per osteoclast remained the same under all conditions, on the calcium phosphate plates coated with rFBN1-N the osteoclasts formed 6-fold more resorption pits, which were significantly smaller in size than control pits (Fig. 1A bottom, C). We next examined how the presence of soluble rFBN1-N or rFBN1-C in the incubation medium affects osteoclast formation. Bone marrow-derived precursors were cultured with MCSF and RANKL or RAW 264.7 cells were cultured with RANKL (50 ng/ ml) for 5–6 days with or without 50 μg/ml rFBN1-N or rFBN1-C, and osteoclast differentiation was quantified. There was no difference in the appearance or numbers of osteoclasts formed in the presence of rFBN1-C compared with positive control (Fig. 1D,E). However, when rFBN1-N was added to the culture medium, osteoclast formation was significantly decreased (Fig. 1D,E). Albumin (50 μg/ml) used as a control to coat calcium phosphate or as a soluble ligand did not affect osteoclast differentiation (supplementary material Fig. S2).

### A small N-terminal fragment of fibrillin-1 acts as an inhibitor of osteoclastogenesis

We used a panel of recombinant sub-fragments spanning rFBN1-N (Fig. 2A) as soluble ligands during osteoclast differentiation from bone marrow or RAW 264.7 cells. The N-terminal half rFBN1-N and rF23, that represents the most N-terminal region of fibrillin-1, significantly inhibited osteoclastogenesis (Fig. 2B; supplementary material Fig.S3A). Expression of RANKL-induced osteoclast marker genes *Ctsk*, *Mmp9* and *Dcstamp* was significantly inhibited by rF23, but not by other fibrillin-1 fragments (Fig. 2C,D;

supplementary material Fig. S3B). The expression of *Trap*, *Rank* and *Itgb3* (integrin β3) was not affected by fibrillin-1 fragments (supplementary material Fig. S3B). rFBN1-N and rF23 inhibited osteoclastogenesis in a dose-dependent manner (supplementary material Fig. S3C) and were most effective when applied for the duration of the experiment (supplementary material Fig. S3D). The inhibitory potential of fibrillin-1 fragments was specific to osteoclasts, since none of the fibrillin-1 fragments affected differentiation of osteoblasts (supplementary material Fig. S4).

### Fibrillin-1 fragments are released during resorption and inhibit osteoclasts *in vivo*

Biotinylated rFBN1-N was coated on calcium phosphate and osteoclastogenesis from bone marrow cells was induced with RANKL and MCSF. Mature osteoclasts were cultured for additional 24 hours in serum free medium, which was then collected and the degradation pattern of fibrillin-1 was visualized by immunoblotting (Fig. 3A). rFBN1-N as well as multiple fibrillin-1 degradation products in the range of 35–85 kDa were released by osteoclasts (Fig. 3A, lane OC). No spontaneous release of biotinylated material was observed when coated wells were incubated without cells (Fig. 3A, lane M). To explore if fibrillin-1 and its degradation products are present in the human bone matrix, we extracted proteins from vertebral bones of healthy individuals. We identified fibrillin-1 multimers, full length fibrillin-1 as well as a number of smaller fibrillin-1 degradation products in the bone tissue (Fig. 3B). To assess if fibrillin-1 degradation fragments can inhibit osteoclast formation in a complex *in vivo* environment, we used a small sub-fragment of rF23, the 32 kDa rF31 (Fig. 3C). We confirmed that similar to rF23, rF31 inhibits osteoclast formation from RAW 264.7 or bone marrow precursors (Fig. 3D). Next, we injected healthy 6-week-old male balb/c mice with rF31 (50 μg/kg) intra-peritoneally every other day for 1 week, and examined 1 week after the last injection osteoclasts in histological sections. In mice injected with rF31 the osteoclast number per bone perimeter was decreased by 50% compared with vehicle-injected animals (Fig. 3E).

### TGFβ does not affect osteoclast formation in the cell culture models used

TGFβ plays a key role in fibrillin-mediated cellular effects in vasculature and bone (Neptune et al., 2003; Nistala et al., 2010b). However, differentiation of RAW 246.7 cells into osteoclasts was not affected by addition of TGFβ1 (1–50 ng/ml) or by inhibition of TGFβ function using a pan-specific TGFβ-neutralizing antibody or an inhibitor of TβRI (supplementary material Fig. S5A,B), indicating that the osteoclastogenesis system used in our study is not sensitive to TGFβ. To exclude that TGFβ co-purified with fibrillin fragments (Kaur and Reinhardt, 2012) may inhibit osteoclastogenesis, we added TGFβ neutralizing antibodies or TβRI inhibitor in the differentiation assays with fibrillin-1 fragments (supplementary material Fig. S5C). Reducing TGFβ levels or signaling did not prevent osteoclast inhibition by rFBN1-N or rF23. Thus, the osteoclast-inhibitory activity exerted by fibrillin-1 fragments in our experimental setup is not mediated by TGFβ.

### The N-terminal half of fibrillin-1 binds and sequesters RANKL

We hypothesized that direct binding of RANKL to fibrillin-1 fragments may mediate their osteoclast inhibitory effects. We performed solid phase binding assays, using RANKL as immobilized and rFBN1-N, rFBN1-C or rF23 as soluble ligands. We confirmed that rFBN1-

N and rF23 are recognized by the detector antibody with similar efficiencies (supplementary material Fig. S6). rFBN1-N, but not rFBN1-C or rF23, interacted with RANKL in a $Ca^{2+}$-dependent manner (Fig. 4A). Furthermore, inhibition of osteoclastogenesis by rFBN1-N was rescued by increasing RANKL levels (Fig. 4B). This strategy was not effective in rescuing osteoclast inhibition induced by rF23 (Fig. 4C).

### rF23 impairs NFATc1 translocation and $Ca^{2+}$ signaling in osteoclast precursors

Since *Ctsk* mRNA expression is regulated by the transcription factor nuclear factor of activated T-cells (NFATc1) (Balkan et al., 2009; Ishida et al., 2002; Takayanagi et al., 2002), we hypothesized that rF23 affects NFATc1 activation. NFATc1 protein expression is induced by RANKL (Ishida et al., 2002; Takayanagi et al., 2002). Inactive hyper-phosphorylated NFATc1 resides in the cytosol. Calcium-dependent phosphatase calcineurin dephosphorylates NFATc1 allowing its nuclear translocation. Osteoclastogenesis from RAW 264.7 cells was induced in the absence or presence of fibrillin-1 fragments and after 3 days NFATc1 levels were monitored. None of the fibrillin-1 fragments affected NFATc1 protein levels (supplementary material Fig. S7). Using immunofluorescence we examined the subcellular localization of NFATc1 (Fig. 5A,B). Nuclear translocation of NFATc1 was prevented by rF23, but was not affected by rFBN1-C or rF18. In the presence of rFBN1-N, a trend of decreased nuclear localization of NFATc1 was observed. To investigate the consequences of fibrillin-1 fragments on cytosolic free $Ca^{2+}$ concentration ($[Ca^{2+}]_i$), RAW 264.7 cells were cultured with RANKL and rFBN1-N, rFBN1-C or rF23 for 3 days, and basal $[Ca^{2+}]_i$ of Fura-2 loaded osteoclast precursors was examined. The $[Ca^{2+}]_i$ in RANKL-treated precursors demonstrated characteristic oscillatory fluctuations (Fig. 5C, top), which were prevented by rF23 (Fig. 5C, bottom). For each cell we quantified the average $[Ca^{2+}]_i$ over 120 seconds of measurement, and the variation in $[Ca^{2+}]_i$ assessed as standard deviation from the average. Plotting average $[Ca^{2+}]_i$ and variation in $[Ca^{2+}]_i$ in the order of ascending basal $[Ca^{2+}]_i$ demonstrated that the cells with higher average $[Ca^{2+}]_i$ also exhibited higher levels of baseline variation (Fig. 5D). Treatment with rF23 resulted in significant decrease in average $[Ca^{2+}]_i$ and in variation of $[Ca^{2+}]_i$ (Fig. 5D,E). rFBN1-C did not affect calcium signaling in osteoclast precursors, but rFBN1-N significantly decreased both average and variation in $[Ca^{2+}]_i$ in osteoclast precursors (Fig. 5E).

## Discussion

In this study, we discovered a novel role of fibrillin-1 in the regulation of osteoclast differentiation. Osteoclastogenesis was found to be negatively regulated by the N-terminal half of fibrillin-1 (rFBN1-N) and by a small 63 kDa fibrillin-1 N-terminal sub-fragment (rF23). This function was specific for osteoclasts and restricted to the application of soluble fibrillin-1 fragments to the apical cell surface. Similar fibrillin-1 fragments were found to be solubilized by the resorptive activity of differentiated osteoclasts. We have identified two differential mechanisms by which fibrillin-1 fragments can inhibit osteoclastogenesis. First, rFBN1-N sequestered RANKL. Second, rF23 prevented calcium fluctuations and NFATc1 translocation in differentiating osteoclasts. The data indicate that osteoclastic degradation of fibrillin-1 might provide a potent negative feedback that limits osteoclast formation and function.

In line with previous studies (Arteaga-Solis et al., 2001; Keene et al., 1991; Kitahama et al., 2000; Quondamatteo et al., 2002; Zhang et al., 1995), we have found that fibrillin-1 and fibrillin-2 are expressed during osteoblast differentiation and secreted into the extracellular matrix. Importantly, we demonstrate that fibrillin-1 is also proteolytically processed during osteoclastic resorption, resulting in several specific degradation products, which were identified in cell culture, as well as in the extracts of human vertebral bone. The significance of our study is that distinct fibrillin-1 fragments are capable of powerful direct inhibition of osteoclastogenesis. The osteoclast inhibitory properties were associated with two different fibrillin-1 sub-fragments, rFBN1-N and rF23. When added as soluble ligands, these proteins strongly inhibited osteoclast differentiation. In contrast, when rFBN1-N was coated on calcium phosphate, it did not affect osteoclast formation, but modulated the resorbing activity. These data suggest that coating fibrillin-1 on the calcium phosphate surface masks the osteoclast-inhibitory epitopes, which become exposed following substrate degradation and solubilization during osteoclastic resorption.

One of the prominent functions of fibrillins is their role in regulating TGFβ and BMPs (Neptune et al., 2003; Nistala et al., 2010b; Sengle et al., 2008). However, we have found that the osteoclastogenesis system used in our study is not sensitive to TGFβ, and that interference with TGFβ levels or signaling minimally affected the osteoclast-inhibitory efficacy of fibrillin-1 fragments. We hypothesized that fibrillin-1 may modulate the bioavailability of RANKL. We have found that rFBN1-N but not rF23 or rFBN1-C, interacts with RANKL in a $Ca^{2+}$-dependent manner, and that inhibition of osteoclastogenesis by rFBN1-N was rescued by increasing RANKL. Based on the differential binding of RANKL to rFBN1-N but not to rF23, the binding site must be located in the region outside of rF23 between EGF4 and cbEGF22. While most fibrillin-1-interacting proteins bind at the N-terminal region comprising rF23, proteoglycans, including perlecan and versican, and heparin/heparan sulfate interact with the central region between EGF4 and cbEGF22 (Isogai et al., 2002; Tiedemann et al., 2001; Tiedemann et al., 2005). In addition to a direct interaction with fibrillin-1, RANKL may also interact with fibrillin-1-bound heparan sulfate, which in turn contributes to RANKL sequestration (Ariyoshi et al., 2008).

We have identified other differences in osteoclastogenesis inhibiting mechanisms between rFBN1-N and rF23, despite the fact that rF23 is fully contained within rFBN1-N. Whereas RANKL-induced gene expression was not affected by rFBN1-N, rF23 selectively inhibited the mRNA expression of proteases cathepsin K and MMP-9, as well as fusion factor Dcstamp. Moreover, calcium/NFATc1 signaling was disturbed to a larger degree by rF23 compared with rFBN1-N. Calcium signaling, which leads to NFATc1 nuclear translocation, is generated by activation of co-stimulatory immune receptors linked to immunoreceptor tyrosine-based activation motif (ITAM)-harboring adaptors (Shinohara et al., 2008). Two ITAM adapter proteins, Fc receptor common c subunit γ (FcRγ) and DNAX-activating protein 12 (DAP12), were identified to be essential for osteoclastogenesis (Koga et al., 2004; Mócsai et al., 2004), and to be coupled to activation of osteoclast-associated immunoglobulin-like receptor (OSCAR) and the triggering receptor expressed in myeloid cells-2 (TREM-2) (Koga et al., 2004; Negishi-Koga and Takayanagi, 2009). Interestingly, OSCAR has been recently identified as a receptor for extracellular matrix proteins, including triple helical collagen I, II and III (Barrow et al., 2011). While we have not identified the

osteoclast receptor for rF23 in this study, it may be possible that OSCAR-induced positive osteoclastogenic signaling is inhibited by rF23.

Modulation of the negative feedback described in our study may contribute to the development of low bone mass in mouse models of MFS, *Fbn1*$^{mgR/mgR}$ (Nistala et al., 2010a), and *Fbn1*$^{-/-}$ (Nistala et al., 2010c), as well as to osteopenia in MFS patients and potentially other type I fibrillinopathies (Giordano et al., 1997). Irrespective of the underlying molecular pathogenetic mechanisms in MFS, including haploinsufficiency, enhanced proteolytic degradation, delayed secretion, and altered proprotein processing, the net effect is a reduced level of fully functional microfibrils in the extracellular matrix and enhanced TGFβ levels (Hubmacher and Reinhardt, 2011). Decreased levels of microfibrils would result in a reduction in the absolute amount of fibrillin-1 degradation fragments generated in bone turnover. This in turn would release the negative feedback controlled by N-terminal fibrillin-1 fragments resulting in enhanced osteoclast formation and activity. MFS mutations typically render fibrillin-1 more susceptible to proteolysis (Kirschner et al., 2011; McGettrick et al., 2000; Reinhardt et al., 2000; Vollbrandt et al., 2004). Cathepsin K cleaves rFBN1-N exclusively in the linker regions between domains producing N-terminal fragments almost identical to the inhibitory rF23 through cleavage sites at Val$^{444}$ and Leu$^{445}$ (Kirschner et al., 2011). In contrast, most of the tested mutations resulted in enhanced degradation within disulfide-bonded loops of individual cbEGF or TB domains. Mutation-mediated cleavage events may also modulate interdomain processing by long-range structural effects that have been reported previously (Kirschner et al., 2011; Vollbrandt et al., 2004). In this regard it is important to note that the rF1F fragment tested in our study fully contains rF23, but lacks osteoclast inhibitory properties, which could be potentially explained by different folding of various length fibrillin-1 fragments. Thus it would be of interest to further validate if MFS mutation-mediated proteolysis of fibrillin-1 may result in degradation products with different conformations, which would in turn cause inappropriate stimulation of osteoclastogenesis.

Taken together with previously published data (Nistala et al., 2010c; Nistala et al., 2010d), our findings suggest a paradigm in which normal bone homeostasis is maintained by fibrillin-1 both indirectly, through regulating TGFβ and RANKL levels, as well as directly by affecting osteoclast formation and function. In MFS and potentially other type I fibrillinopathies, the following consequences may occur: (1) TGFβ levels produced by osteoblasts increase and induce RANKL expression (Nistala et al., 2010d), (2) compromised sequestration of RANKL by mutated fibrillin-1 additionally increases RANKL levels, and (3) production of small N-terminal inhibitory fragments is decreased either due to overall decrease in fibrillin-1 or due to its abnormal degradation. All these additive mechanisms result in elevated osteoclastogenesis and osteopenia.

## Materials and Methods

### Recombinant proteins, cytokines and growth factors

Recombinant fragments of human fibrillin-1, rFBN1-N (rF16), rFBN1-C (rF6H), rF18, rF23, rF1F, rF31 and rF51, were produced as described previously (El-Hallous et al., 2007; Jensen et al., 2001; Keene et al., 1997; Reinhardt et al., 1996a; Reinhardt et al., 1996b),

diluted at 50 μg/ml in 50 mM Tris-HCl, pH 7.4, 150 mM NaCl (TBS) including 2 mM $CaCl_2$. TGFβ1 (1–50 ng/ml) was from Invitrogen (PHG9204), TGFβ neutralizing antibody (15 μg/ml) was from R&D (AB-100-NA) and TβRI inhibitor (5 μM) was from Sigma (SB 431542). Recombinant GST-RANKL was purified from clones kindly provided by Dr M. F. Manolson (University of Toronto) (Manolson et al., 2003). MCSF was from Peprotech (300-25). For biotinylation, rFBN1-N was dialyzed in 20 mM HEPES, pH 7.4, 500 mM NaCl, 2.5 mM $CaCl_2$ and biotinylated using EZ-Link Sulfo-NHS-LC-Biotin (Thermo Scientific; 21335).

## Osteoclast cultures

The mouse monocytic cell line RAW 264.7 obtained from the American Tissue Culture Collection (ATCC; TIB-71) was cultured in DMEM (Wisent; 319-020-CL) with 10% fetal bovine serum (FBS) (Wisent; 080152), 1 mM pyruvate (Wisent; 600-110-EL), and 1% penicillin, streptomycin, L-glutamine solution (Wisent; 450-202-EL). To generate osteoclasts, RAW 264.7 cells were plated at $5\times10^3$ cells/$cm^2$ and grown with RANKL (50 ng/ml) for 5–7 days with one medium change on day 3.

Studies were compliant with McGill University guidelines established by the Canadian Council on Animal Care. Mouse bone marrow was isolated as described previously (Hussein et al., 2011). Bone marrow cells were incubated overnight in αMEM (Wisent; 310-022-CL) supplemented with 10% FBS, 1 mM pyruvate, 1% penicillin, streptomycin, L-glutamine solution and 50 ng/ml MCSF. Non-adherent cells were harvested, plated at $5\times10^4$ cells/$cm^2$ and grown with MCSF (50 ng/ml) and RANKL (50 ng/ml) for 5–7 days with one medium change on day 3.

Cultures were fixed with 10% formalin and stained for TRAP (Sigma; 387A-KT). Osteoclasts were identified as TRAP-positive cells with three or more nuclei.

## Extraction of human bone

Vertebrae from a 16-year-old female were obtained with consent through the Transplant Quebec Organ Donation Program, and stored at −70°C. Proteins were extracted from the mineralized bone matrix as described previously (Dickson and Roughley, 1993). Briefly, the bone was powdered, treated with 4 M guanidinium chloride to remove proteins present in soft connective tissues, then bone powder was treated with 4 M guanidinium chloride containing 0.2 M EDTA to extract proteins from the mineralized matrix. Proteins in the extract were precipitated with 9 volumes of ethanol and used directly for analysis by SDS-PAGE. Fibrillin-1 was immunoblotted using primary polyclonal antibody against rFBN1-N (1:100) (Lin et al., 2002).

## Osteoclastic resorption

Osteoassay plates (Corning; 3989) were preincubated with complete medium and 50 μg/ml of rFBN1-N, rFBN1-C or BSA overnight at 37°C. To quantify resorption, the cells were removed with 10% NaClO, the wells were washed with water and air dried. Resorption pits were measured using PixeLINK Capture SE software.

### Animal model

Studies were compliant with McGill University guidelines established by the Canadian Council on Animal Care. Male Balb/c mice (6 weeks) were injected intra-peritoneally with vehicle (PBS, $n$=11) or 50 μg/kg of rF31 ($n$=4) every other day for 1 week. The mice were euthanized 1 week after the last injection, and hind limbs were dissected immediately. Tibias were decalcified in EDTA, embedded in paraffin, sectioned (5 μm thickness) and stained for TRAP in the histology platform of the Centre for Bone and Periodontal Research, McGill University. TRAP-positive cells were counted 100 μm below the growth plate, in two fields per mouse using Osteomeasure 3.0 (Osteometrics).

### Quantitative real-time PCR (qPCR)

Total RNA was isolated as described previously (Guo et al., 2008; Hussein et al., 2011), quantified with a Quant-iT instrument (Invitrogen; #Q32860) and reverse transcribed using the High Capacity cDNA Reverse Transcription Kit (Life Technologies; #4368814). PCR was performed with a 7500 Applied Biosystem instrument using TaqMan probes with the universal PCR Master Mix (Life Technologies), or SYBR Green primers and PCR Master Mix (Hoffmann-La Roche Ltd) in a total volume of 25 μl including 0.9 μM of reverse and forward primers from Life Technologies. The following probes were used: Taqman: *Ctsk* (Cathepsin K): Mm00484039_m1; *Mmp9* (Matrix metalloprotease 9): Mm00600163_m1; *Fbn1* (Fibrillin-1): Mm00514908_m1; *Fbn2* (Fibrillin-2): Mm00515742_m1; *Tnfrsf11a* (Rank): Mm00437132_m1; *Acp5* (Trap): Mm00475698_m1; *Sp7* (Osterix): Mm00504574_m1; *Col1a1* (Collagen I alpha 1): Mm00801666_g1; *Gapdh* (Glyceraldehyde 3-phosphate dehydrogenase): Mm99999915_g1. SYBR Green (forward, reverse): *Itgb3* (Integrin β3): (TCCAGACCCTGGGTACCAAG, GCCAATCCGAAGGTTGCTAG); *Dcstamp* (Dendritic cell-specific transmembrane protein): (CTTCCGTGGGCCAGAAGTT, AGGCCAGTGCTGACTAGGATGA); *Opn* (Osteopontin): (GTGGACTC-GGATGAATCTG, TCGACTGTAGGGACGATTG); *Runx2* (Runt-related transcription factor 2): (TGGCTTGGGTTTCAGGTTAG, TCGGTTTCTTAGG-GTCTTGGA); *Gapdh*: (CAAGTATGATGACATCAAGAAGGTGG, GGAAGA-GTGGGAGTTGCTGTTG).

### Immunoblotting

Whole cell lysates were prepared as described previously (Tiedemann et al., 2009). Briefly, the cells were lysed using a RIPA buffer (50 mM Tris-HCl, pH 7.4, 150 mM NaCl, 1% Nonidet P-40, 1 mM EDTA, 10 mg/ml aprotinin, 1 mg/ml leupeptin, 0.1 M phenylmethylsulfonyl fluoride, 0.5 M sodium fluoride and 1 mM sodium orthovanadate). The protein concentrations were determined using a Quant-iT protein assay kit (Invitrogen). Conditioned media were collected and filtered using a 0.22 μm filter, aliquots were kept at −80°C. Proteins (50 μg) were precipitated in 10% trichloroacetic acid, redissolved in 1× SDS sample buffer, separated by 7.5% gel electrophoresis under reducing conditions, transferred to a nitrocellulose membrane (Bio-Rad, #162-0115; 0.45 μm) using 10 mM sodium borate, pH 8.9, blocked in 5% non-fat milk in TBST buffer (10 mM Tris-HCl, pH 7.5, 150 mM NaCl, 0.05% Tween 20) for 1 h at 4°C followed by overnight incubation at 4°C with the primary antibodies: NFATc1 (1:100, sc-7294, Santa Cruz Biotechnology), tubulin (1:5000, T6793, Sigma), hexahistidine tag (1:5,000, R930-25, Invitrogen); rFBN1-N

(1:100), rFBN1-C (1:250), rFBN2-C (1:250) (Lin et al., 2002; Tiedemann et al., 2001; Tiedemann et al., 2005); then with horseradish peroxidase-conjugated secondary antibodies (1:200–1:10,000, Bio-Rad; goat anti-mouse, #170-5047; goat anti-rabbit #170-5046) or NeutrAvidin horseradish peroxidase conjugate (Thermo Scientific, #31001, 1:800) and visualized using a chemiluminescence substrate (Thermo Scientific, #32106).

### Immunofluorescence

Immunostaining for NFATc1 was performed as described previously (Guo et al., 2008). Briefly, osteoclasts on glass coverslips were fixed with 10% formalin, incubated with mouse anti-NFATc1 antibody (1:100, Santa Cruz Biotechnology; #SC-7294), followed by a biotinylated goat anti-mouse IgG (1:200, Invitrogen; # A10519) and Alexa-Fluor-488-conjugated streptavidin (1:500, Invitrogen; #S-11223). Nuclei were counterstained using 4′, 6-diamidino-2-phenylindole dihydrochloride (DAPI; 1:10,000, Invitrogen; #D1306). For each experiment, five random images per condition were recorded. NFATc1 localization was considered nuclear when the fluorescence intensity of nuclei exceeded that of the cytoplasm.

Osteoblasts were fixed with 10% formalin, and immunofluorescence of fibrillin-1 and fibrillin-2 was performed as described previously with primary antibodies against rFBN1-C (1:100) and rFBN2-C (1:100) (Lin et al., 2002; Tiedemann et al., 2001; Tiedemann et al., 2005).

### Solid-phase binding assay

Solid-phase binding assays were performed as described previously (Lin et al., 2002). Briefly, 96-well plates (MaxiSorp, Nalge Nunc International) were coated overnight in 4°C with RANKL (20 μg/ml) in TBS or TBS alone, and blocked for 1 hour with 5% (w/v) non-fat milk in TBS. rFBN1-N, rFBN1-C or rF23 were incubated as soluble ligands (0–150 μg/ml) in TBS with 5% non-fat milk, with either 5 mM $CaCl_2$ or 10 mM EDTA at room temperature, and washed with TBS containing 0.05% (v/v) Tween 20. The wells were incubated for 1 hour with the primary antibody against rFBN1-N [1:250, (Lin et al., 2002)], followed by horseradish-peroxidase-conjugated secondary goat anti-rabbit antibody (1:800 diluted; Bio-Rad) for 1 hour. Color development was performed with 1 mg/ml 5-aminosalicylic acid (Sigma) in 20 mM phosphate buffer, pH 6.8, including 0.1% $H_2O_2$ for 3–5 minutes, stopped with 2 M NaOH, and measured at 492 nm using a Microplate reader. OD measured in control wells (blocked with non-fat milk, but without immobilized ligand) were subtracted from all measured values.

### Microspectrofluorometry

Cells plated onto glass-bottom 35 mm dishes (MatTek.) were loaded with Fura-2-AM (Invitrogen; F1221) at room temperature for 40 minutes and changes in $[Ca^{2+}]_i$ were measured for 120 seconds, as described previously (Tiedemann et al., 2009). $[Ca^{2+}]_i$ values were calculated using a Fura-2-AM calcium imaging calibration kit (Invitrogen; F6774).

### Statistics

Data are presented as means ± standard error of the mean (s.e.m.) with sample size ($n$) indicating the number of independent experiments, or as means ± standard deviation (s.d.)

with sample size ($n$) indicating the number of samples. Differences were assessed by ANOVA or Student's $t$-test and accepted as statistically significant at $P<0.05$.

## Acknowledgments

We are grateful to Dr Morris F. Manolson for providing GST-RANKL clones and to Dr Lisbet Haglund for preparing the human bone sample, and to Ms Amelie Pagliuzza for performing a control ELISA and Ms Meng Lan Li for helping with histomorphometric analysis.

**Funding**

This work was supported by the Canadian Institutes of Health Research [grant number MOP-106494 to D.P.R. and MOP-77643 to S.V.K.]; the Réseau de recherche en santé buccodentaire et osseuse; the Natural Sciences and Engineering Research Council of Canada [grant number RGPIN 375738-09]. D.P.R. holds a Canada Research Chair in Cell-Matrix Biology and S.V.K. holds a Canada Research Chair in Osteoclast Biology.

## References

Ariyoshi W, Takahashi T, Kanno T, Ichimiya H, Shinmyouzu K, Takano H, Koseki T, Nishihara T. Heparin inhibits osteoclastic differentiation and function. J Cell Biochem. 2008; 103:1707–1717. [PubMed: 18231993]

Arteaga-Solis E, Gayraud B, Lee SY, Shum L, Sakai L, Ramirez F. Regulation of limb patterning by extracellular microfibrils. J Cell Biol. 2001; 154:275–281. [PubMed: 11470817]

Balkan W, Martinez AF, Fernandez I, Rodriguez MA, Pang M, Troen BR. Identification of NFAT binding sites that mediate stimulation of cathepsin K promoter activity by RANK ligand. Gene. 2009; 446:90–98. [PubMed: 19563866]

Barrow AD, Raynal N, Andersen TL, Slatter DA, Bihan D, Pugh N, Cella M, Kim T, Rho J, Negishi-Koga T, et al. OSCAR is a collagen receptor that costimulates osteoclastogenesis in DAP12-deficient humans and mice. J Clin Invest. 2011; 121:3505–3516. [PubMed: 21841309]

Carter N, Duncan E, Wordsworth P. Bone mineral density in adults with Marfan syndrome. Rheumatology (Oxford). 2000; 39:307–309. [PubMed: 10788540]

Dickson IR, Roughley PJ. The effects of vitamin D deficiency on proteoglycan and hyaluronate constituents of chick bone. Biochim Biophys Acta. 1993; 1181:15–22. [PubMed: 8457600]

Doyle JJ, Gerber EE, Dietz HC. Matrix-dependent perturbation of TGFβ signaling and disease. FEBS Lett. 2012; 586:2003–2015. [PubMed: 22641039]

El-Hallous E, Sasaki T, Hubmacher D, Getie M, Tiedemann K, Brinckmann J, Bätge B, Davis EC, Reinhardt DP. Fibrillin-1 interactions with fibulins depend on the first hybrid domain and provide an adaptor function to tropoelastin. J Biol Chem. 2007; 282:8935–8946. [PubMed: 17255108]

Giannoudis PV, Kanakaris NK, Einhorn TA. Interaction of bone morphogenetic proteins with cells of the osteoclast lineage: review of the existing evidence. Osteoporos Int. 2007; 18:1565–1581. [PubMed: 17694399]

Giordano N, Senesi M, Battisti E, Mattii G, Gennari C. Weill-Marchesani syndrome: report of an unusual case. Calcif Tissue Int. 1997; 60:358–360. [PubMed: 9075633]

Grahame R, Pyeritz RE. The Marfan syndrome: joint and skin manifestations are prevalent and correlated. Br J Rheumatol. 1995; 34:126–131. [PubMed: 7704457]

Guo Y, Tiedemann K, Khalil JA, Russo C, Siegel PM, Komarova SV. Osteoclast precursors acquire sensitivity to breast cancer derived factors early in differentiation. Bone. 2008; 43:386–393. [PubMed: 18502714]

Hubmacher, D., Reinhardt, DP. Microfibrils and fibrillin. In: Mecham, RP., editor. Biology of Extracellular Matrix. New York, NY: Springer; 2011. p. 233-265.

Hubmacher D, Tiedemann K, Reinhardt DP. Fibrillins: from biogenesis of microfibrils to signaling functions. Curr Top Dev Biol. 2006; 75:93–123. [PubMed: 16984811]

Hussein O, Tiedemann K, Komarova SV. Breast cancer cells inhibit spontaneous and bisphosphonate-induced osteoclast apoptosis. Bone. 2011; 48:202–211. [PubMed: 20849994]

Ishida N, Hayashi K, Hoshijima M, Ogawa T, Koga S, Miyatake Y, Kumegawa M, Kimura T, Takeya T. Large scale gene expression analysis of osteoclastogenesis in vitro and elucidation of NFAT2 as a key regulator. J Biol Chem. 2002; 277:41147–41156. [PubMed: 12171919]

Isogai Z, Aspberg A, Keene DR, Ono RN, Reinhardt DP, Sakai LY. Versican interacts with fibrillin-1 and links extracellular microfibrils to other connective tissue networks. J Biol Chem. 2002; 277:4565–4572. [PubMed: 11726670]

Janssens K, ten Dijke P, Janssens S, Van Hul W. Transforming growth factor-beta1 to the bone. Endocr Rev. 2005; 26:743–774. [PubMed: 15901668]

Jensen SA, Reinhardt DP, Gibson MA, Weiss AS. Protein interaction studies of MAGP-1 with tropoelastin and fibrillin-1. J Biol Chem. 2001; 276:39661–39666. [PubMed: 11481325]

Kaur J, Reinhardt DP. Immobilized metal affinity chromatography co-purifies TGF-β1 with histidine-tagged recombinant extracellular proteins. PLoS ONE. 2012; 7:e48629. [PubMed: 23119075]

Keene DR, Sakai LY, Burgeson RE. Human bone contains type III collagen, type VI collagen, and fibrillin: type III collagen is present on specific fibers that may mediate attachment of tendons, ligaments, and periosteum to calcified bone cortex. J Histochem Cytochem. 1991; 39:59–69. [PubMed: 1983874]

Keene DR, Jordan CD, Reinhardt DP, Ridgway CC, Ono RN, Corson GM, Fairhurst M, Sussman MD, Memoli VA, Sakai LY. Fibrillin-1 in human cartilage: developmental expression and formation of special banded fibers. J Histochem Cytochem. 1997; 45:1069–1082. [PubMed: 9267468]

Kirschner R, Hubmacher D, Iyengar G, Kaur J, Fagotto-Kaufmann C, Brömme D, Bartels R, Reinhardt DP. Classical and neonatal Marfan syndrome mutations in fibrillin-1 cause differential protease susceptibilities and protein function. J Biol Chem. 2011; 286:32810–32823. [PubMed: 21784848]

Kitahama S, Gibson MA, Hatzinikolas G, Hay S, Kuliwaba JL, Evdokiou A, Atkins GJ, Findlay DM. Expression of fibrillins and other microfibril-associated proteins in human bone and osteoblast-like cells. Bone. 2000; 27:61–67. [PubMed: 10865210]

Koga T, Inui M, Inoue K, Kim S, Suematsu A, Kobayashi E, Iwata T, Ohnishi H, Matozaki T, Kodama T, et al. Costimulatory signals mediated by the ITAM motif cooperate with RANKL for bone homeostasis. Nature. 2004; 428:758–763. [PubMed: 15085135]

Kohlmeier L, Gasner C, Bachrach LK, Marcus R. The bone mineral status of patients with Marfan syndrome. J Bone Miner Res. 1995; 10:1550–1555. [PubMed: 8686512]

Le Goff C, Cormier-Daire V. From tall to short: the role of TGFβ signaling in growth and its disorders. Am J Med Genet C Semin Med Genet. 2012; 160C:145–153. [PubMed: 22791552]

Le Parc JM, Plantin P, Jondeau G, Goldschild M, Albert M, Boileau C. Bone mineral density in sixty adult patients with Marfan syndrome. Osteoporos Int. 1999; 10:475–479. [PubMed: 10663348]

Lin G, Tiedemann K, Vollbrandt T, Peters H, Batge B, Brinckmann J, Reinhardt DP. Homo- and heterotypic fibrillin-1 and -2 interactions constitute the basis for the assembly of microfibrils. J Biol Chem. 2002; 277:50795–50804. [PubMed: 12399449]

Manolson MF, Yu H, Chen W, Yao Y, Li K, Lees RL, Heersche JN. The a3 isoform of the 100-kDa V-ATPase subunit is highly but differentially expressed in large (>or=10 nuclei) and small (<or= nuclei) osteoclasts. J Biol Chem. 2003; 278:49271–49278. [PubMed: 14504271]

McGettrick AJ, Knott V, Willis A, Handford PA. Molecular effects of calcium binding mutations in Marfan syndrome depend on domain context. Hum Mol Genet. 2000; 9:1987–1994. [PubMed: 10942427]

Mócsai A, Humphrey MB, Van Ziffle JA, Hu Y, Burghardt A, Spusta SC, Majumdar S, Lanier LL, Lowell CA, Nakamura MC. The immunomodulatory adapter proteins DAP12 and Fc receptor gamma-chain (FcRgamma) regulate development of functional osteoclasts through the Syk tyrosine kinase. Proc Natl Acad Sci USA. 2004; 101:6158–6163. [PubMed: 15073337]

Moura B, Tubach F, Sulpice M, Boileau C, Jondeau G, Muti C, Chevallier B, Ounnoughene Y, Le Parc JM. Multidisciplinary Marfan Syndrome Clinic Group. Bone mineral density in Marfan syndrome. A large case-control study. Joint Bone Spine. 2006; 73:733–735. [PubMed: 17056292]

Negishi-Koga T, Takayanagi H. Ca2+-NFATc1 signaling is an essential axis of osteoclast differentiation. Immunol Rev. 2009; 231:241–256. [PubMed: 19754901]

Neptune ER, Frischmeyer PA, Arking DE, Myers L, Bunton TE, Gayraud B, Ramirez F, Sakai LY, Dietz HC. Dysregulation of TGF-beta activation contributes to pathogenesis in Marfan syndrome. Nat Genet. 2003; 33:407–411. [PubMed: 12598898]

Nistala H, Lee-Arteaga S, Carta L, Cook JR, Smaldone S, Siciliano G, Rifkin AN, Dietz HC, Rifkin DB, Ramirez F. Differential effects of alendronate and losartan therapy on osteopenia and aortic aneurysm in mice with severe Marfan syndrome. Hum Mol Genet. 2010a; 19:4790–4798. [PubMed: 20871099]

Nistala H, Lee-Arteaga S, Siciliano G, Smaldone S, Ramirez F. Extracellular regulation of transforming growth factor beta and bone morphogenetic protein signaling in bone. Ann N Y Acad Sci. 2010b; 1192:253–256. [PubMed: 20392244]

Nistala H, Lee-Arteaga S, Smaldone S, Siciliano G, Carta L, Ono RN, Sengle G, Arteaga-Solis E, Levasseur R, Ducy P, et al. Fibrillin-1 and -2 differentially modulate endogenous TGF-β and BMP bioavailability during bone formation. J Cell Biol. 2010c; 190:1107–1121. [PubMed: 20855508]

Nistala H, Lee-Arteaga S, Smaldone S, Siciliano G, Ramirez F. Extracellular microfibrils control osteoblast-supported osteoclastogenesis by restricting TGFbeta stimulation of RANKL production. J Biol Chem. 2010d; 285:34126–34133. [PubMed: 20729550]

Pyeritz RE. The Marfan syndrome. Annu Rev Med. 2000; 51:481–510. [PubMed: 10774478]

Quinn JM, Itoh K, Udagawa N, Hausler K, Yasuda H, Shima N, Mizuno A, Higashio K, Takahashi N, Suda T, et al. Transforming growth factor beta affects osteoclast differentiation via direct and indirect actions. J Bone Miner Res. 2001; 16:1787–1794. [PubMed: 11585342]

Quondamatteo F, Reinhardt DP, Charbonneau NL, Pophal G, Sakai LY, Herken R. Fibrillin-1 and fibrillin-2 in human embryonic and early fetal development. Matrix Biol. 2002; 21:637–646. [PubMed: 12524050]

Ramirez F, Sakai LY, Rifkin DB, Dietz HC. Extracellular microfibrils in development and disease. Cell Mol Life Sci. 2007; 64:2437–2446. [PubMed: 17585369]

Reinhardt DP, Keene DR, Corson GM, Pöschl E, Bächinger HP, Gambee JE, Sakai LY. Fibrillin-1: organization in microfibrils and structural properties. J Mol Biol. 1996a; 258:104–116. [PubMed: 8613981]

Reinhardt DP, Sasaki T, Dzamba BJ, Keene DR, Chu ML, Göhring W, Timpl R, Sakai LY. Fibrillin-1 and fibulin-2 interact and are colocalized in some tissues. J Biol Chem. 1996b; 271:19489–19496. [PubMed: 8702639]

Reinhardt DP, Ono RN, Notbohm H, Müller PK, Bächinger HP, Sakai LY. Mutations in calcium-binding epidermal growth factor modules render fibrillin-1 susceptible to proteolysis. A potential disease-causing mechanism in Marfan syndrome. J Biol Chem. 2000; 275:12339–12345. [PubMed: 10766875]

Sabatier L, Miosge N, Hubmacher D, Lin G, Davis EC, Reinhardt DP. Fibrillin-3 expression in human development. Matrix Biol. 2011; 30:43–52. [PubMed: 20970500]

Sengle G, Charbonneau NL, Ono RN, Sasaki T, Alvarez J, Keene DR, Bächinger HP, Sakai LY. Targeting of bone morphogenetic protein growth factor complexes to fibrillin. J Biol Chem. 2008; 283:13874–13888. [PubMed: 18339631]

Shinohara M, Koga T, Okamoto K, Sakaguchi S, Arai K, Yasuda H, Takai T, Kodama T, Morio T, Geha RS, et al. Tyrosine kinases Btk and Tec regulate osteoclast differentiation by linking RANK and ITAM signals. Cell. 2008; 132:794–806. [PubMed: 18329366]

Takayanagi H, Kim S, Koga T, Nishina H, Isshiki M, Yoshida H, Saiura A, Isobe M, Yokochi T, Inoue J, et al. Induction and activation of the transcription factor NFATc1 (NFAT2) integrate RANKL signaling in terminal differentiation of osteoclasts. Dev Cell. 2002; 3:889–901. [PubMed: 12479813]

Tiedemann K, Bätge B, Müller PK, Reinhardt DP. Interactions of fibrillin-1 with heparin/heparan sulfate, implications for microfibrillar assembly. J Biol Chem. 2001; 276:36035–36042. [PubMed: 11461921]

Tiedemann K, Sasaki T, Gustafsson E, Göhring W, Bätge B, Notbohm H, Timpl R, Wedel T, Schlötzer-Schrehardt U, Reinhardt DP. Microfibrils at basement membrane zones interact with perlecan via fibrillin-1. J Biol Chem. 2005; 280:11404–11412. [PubMed: 15657057]

Tiedemann K, Hussein O, Sadvakassova G, Guo Y, Siegel PM, Komarova SV. Breast cancer-derived factors stimulate osteoclastogenesis through the Ca2+/protein kinase C and transforming growth factor-beta/MAPK signaling pathways. J Biol Chem. 2009; 284:33662–33670. [PubMed: 19801662]

Vollbrandt T, Tiedemann K, El-Hallous E, Lin G, Brinckmann J, John H, Bätge B, Notbohm H, Reinhardt DP. Consequences of cysteine mutations in calcium-binding epidermal growth factor modules of fibrillin-1. J Biol Chem. 2004; 279:32924–32931. [PubMed: 15161917]

Zhang H, Hu W, Ramirez F. Developmental expression of fibrillin genes suggests heterogeneity of extracellular microfibrils. J Cell Biol. 1995; 129:1165–1176. [PubMed: 7744963]

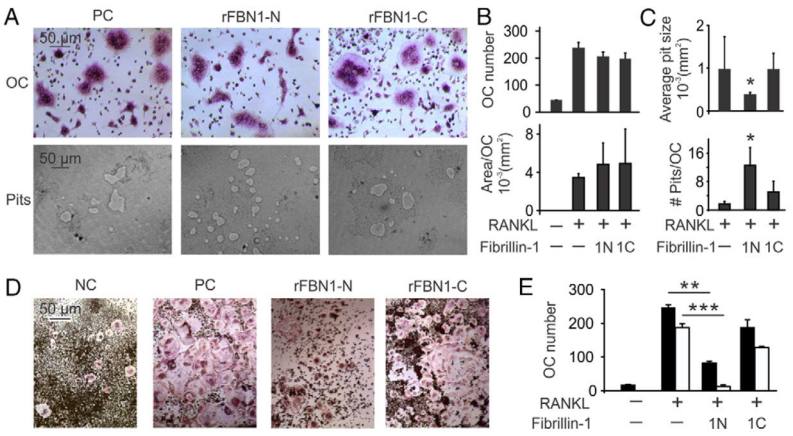


**Fig. 1. The N-terminal half of fibrillin-1 affects osteoclastic resorption and inhibits osteoclast differentiation**

(A–C) Bone marrow cells were plated on calcium phosphate that was uncoated (positive control, PC) or coated with 50 μg/ml rFBN1-N (1N) or rFBN1-C (1C) and differentiation was induced with MCSF (50 ng/ml) and RANKL (50 ng/ml). After 5–6 days the samples were fixed and stained for TRAP. Osteoclasts were quantified, removed and resorption was assessed. (A) Representative images of osteoclasts (top) and resorption pits (bottom) formed under the indicated conditions. Scale bars apply to all images in the corresponding rows. (B,C) Average numbers of differentiated osteoclasts (B, top), total area resorbed per osteoclast (B, bottom), average pit size (C, top), and numbers of resorption pits per osteoclast (C, bottom). Data are means ± s.e.m., $n$=3 experiments; *$P$<0.05 assessed by Student's $t$-test. (D,E) Bone marrow cells [white bars, all conditions treated with MCSF (50 ng/ml)] or RAW 264.7 (black bars) were cultured for 5 days without RANKL (negative control, NC); with RANKL (50 ng/ml, positive control, PC) or with RANKL and soluble rFBN1-N or rFBN1-C, fixed and stained for TRAP. (D) Representative images of osteoclastic cells formed from RAW 264.7 under the indicated conditions. Scale bars apply to all images. (E) Average numbers of osteoclasts. Data are means ± s.e.m., $n$=4 experiments for bone marrow cells, $n$=5–6 experiments for RAW 264.7; **$P$<0.01, ***$P$<0.001 assessed by Student's $t$-test.

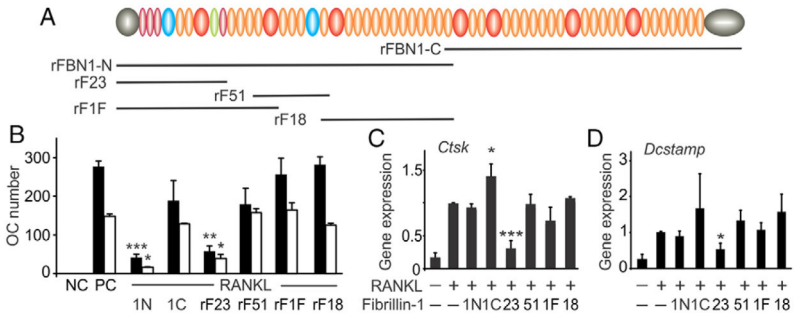


**Fig. 2. A small N-terminal subfragment of fibrillin-1 inhibits osteoclastogenesis**

(A) Schematic of recombinant N-terminal (rFBN1-N) and C-terminal (rFBN1-C) halves of fibrillin-1, and recombinant sub-fragments of rFBN1-N – rF23, rF51, rF1F and rF18. (B–D) Bone marrow cells (white bars) and RAW 264.7 (black bars) were cultured for 5 days untreated (negative control, NC), treated with RANKL only (50 ng/ml, positive control, PC) or treated with RANKL and 50 μg/ml of soluble fibrillin-1 fragments rFBN1-N, rFBN1-C, rF23, rF51, rF1F or rF18. (B) Average numbers of osteoclasts formed under the indicated conditions. Data are means ± s.e.m., $n$=3–8 experiments; *$P$<0.05, **$P$<0.01, ***$P$<0.001 compared with PC assessed by Student's $t$-test. (C,D) mRNA was isolated and the expression of cathepsin K (*Ctsk*, C) and *Dcstamp* (D) was quantified. Data are means ± s.e.m., $n$=3–9 experiments; *$P$<0.05, ***$P$<0.001, compared with PC assessed by Student's $t$-test.

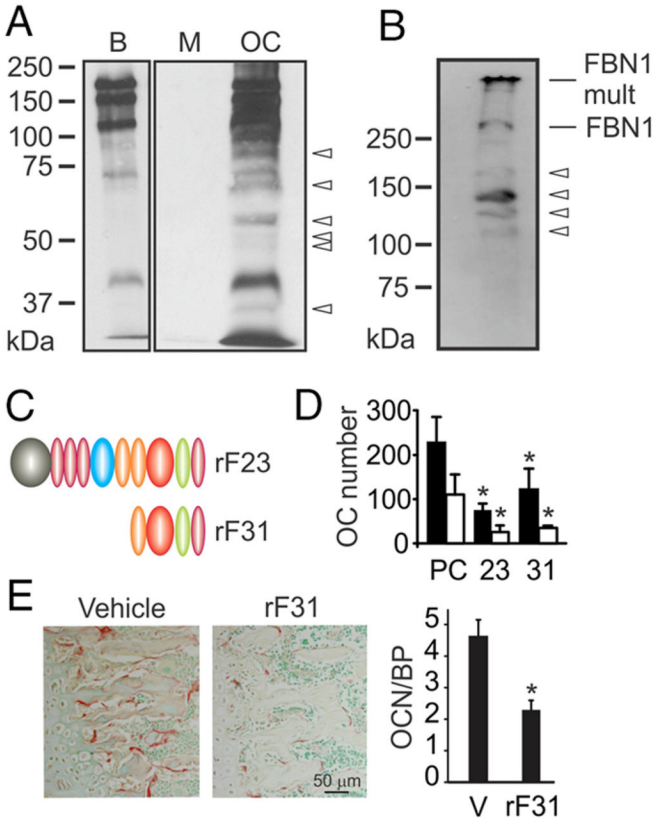


**Fig. 3. Fragments of fibrillin-1 are released during resorption and inhibit osteoclasts *in vivo***

(A) Bone marrow cells were plated on calcium phosphate coated with biotinylated rFBN1-N (80–155 µg/cm$^2$) and after mature osteoclasts developed (5–7 days), the cultures were maintained for an additional 24 hours in serum free medium. Lane B, Biotinylated rFBN1-N before coating. Lane OC, conditioned medium from wells cultured with osteoclasts. Lane M, conditioned medium from wells cultured identically, but without cells. Arrowheads indicate degradation products in the range of 35–85 kDa. (B) Proteins were extracted from human vertebral bone and immunoblotted for fibrillin-1. Arrows indicate multimeric (FBN1 mult.) and monomeric full length fibrillin-1 (FBN1); arrowheads indicate fibrillin-1 degradation products. (C) Schematic of recombinant sub-fragments rF23 and rF31 (compare with Fig. 2 for position within full length fibrillin-1). (D) Bone marrow cells (white bars) and RAW 264.7 (black bars) were cultured in parallel for 5 days with RANKL only (50 ng/ml, positive control, PC), or with RANKL and 50 µg/ml of rF23 or rF31. Data are means ± s.e.m., $n$=2–3 experiments; *$P$<0.05, compared with PC assessed by Student's $t$-test. (E) Healthy mice were injected with vehicle (PBS) or recombinant rF31 (50 µg/kg) intra-peritoneally every other day for 1 week and osteoclast numbers were assessed 1 week after the last injection. Left, representative images of upper tibial metaphyseal area of vehicle- or rF31-treated mice. Right, osteoclast number (OCN) per bone perimeter (BP) in vehicle- and rF31-injected mice. Data are means ± s.d., $n$=11 mice for vehicle-injected and $n$=4 mice for rF31-injected; *$P$<0.05, assessed by Student's $t$-test.

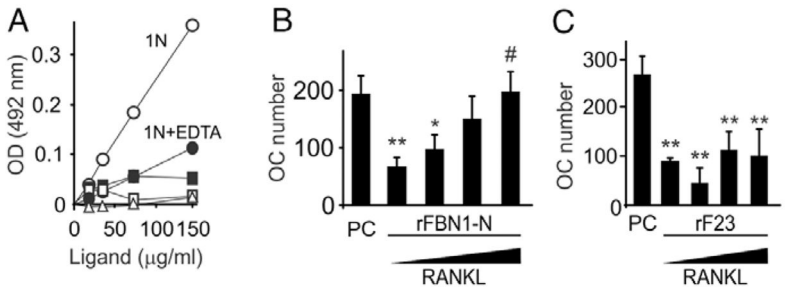


**Fig. 4. The N-terminal half of fibrillin-1 binds and sequesters RANKL**

(A) rFBN1-N (circles), but not rFBN1-C (squares) or rF23 (triangles), binds RANKL. RANKL (20 μg/ml) was immobilized and rFBN1-N, rFBN1-C or rF23 (0–150 μg/ml) were added as soluble ligands, in $Ca^{2+}$-containing (open symbols) or $Ca^{2+}$-free (filled symbols) buffer, and bound proteins were detected. Non-specific binding to milk proteins without coated RANKL was subtracted from all values. Data are representative of three independent experiments. (B,C) RAW 264.7 cells were incubated with 50 μg/ml of rFBN1-N (B) or rF23 (C) and increasing concentrations of RANKL (0.1, 1, 3 and 10 μg/ml), and osteoclast numbers were assessed. Data in B are means ± s.e.m., $n$=3–5 experiments, *$P$<0.05 and **$P$<0.01 indicate significance compared with PC; #$P$<0.05 indicates significance compared with the rFBN1-N treated sample including 0.1 μg/ml RANKL, as analyzed by ANOVA. Data in C are means ± s.e.m., $n$=4 experiments; **$P$<0.01 compared with PC, as assessed by ANOVA.

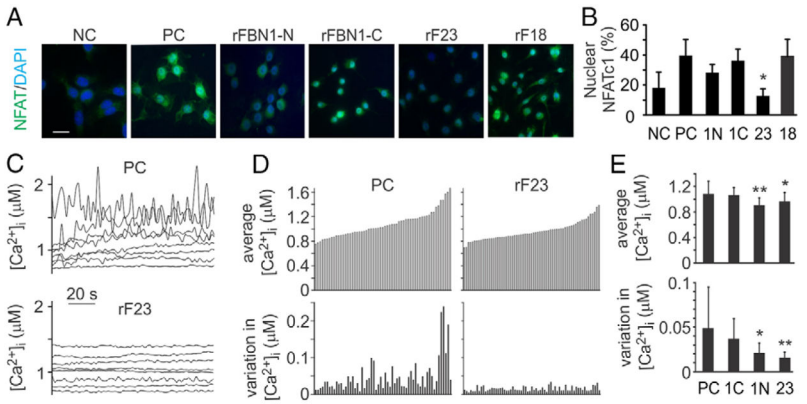


**Fig. 5. Fibrillin-1 fragments act through the $Ca^{2+}$–NFATc1 pathway**

RAW 264.7 cells were cultured untreated (negative control, NC), treated with RANKL (positive control, PC) or RANKL and 50 μg/ml of rFBN1-N (1N), rFBN1-C (1C), rF23 (23) or rF18 (18) for 48 hours. (A) NFATc1 localization was determined by immunofluorescence (green). Nuclei were counterstained using DAPI (blue). Scale bar: 100 μm. (B) The percentage of cells exhibiting nuclear NFATc1 of the total number of cells. Data are means ± s.d.; $n$=220 cells for positive control, $n$=137 cells for rFBN1-N-treated, $n$=282 cells for rFBN1-C-treated, $n$=135 cells for rF23-treated and $n$=117 cells for rF18-treated samples; *$P$<0.05 assessed by Student's $t$-test. (C–E) Osteoclast precursors were loaded with Fura-2AM, and $[Ca^{2+}]_i$ was monitored for 120 seconds. (C) Representative traces demonstrate changes in $[Ca^{2+}]_i$ in eight individual cells per experimental condition. (D) For each cell, the average $[Ca^{2+}]_i$ (top) and variation in baseline $[Ca^{2+}]_i$, measured as a standard deviation of basal levels (bottom) were determined and presented in an ascending order of the average $[Ca^{2+}]_i$; $n$=59 cells for positive control, $n$=65 cells for rF23-treated samples. (E) Average $[Ca^{2+}]_i$ (top) and variation in $[Ca^{2+}]_i$ (bottom). Data are means ± s.d.; $n$=59 cells for PC, $n$=65 for rFBN1-C-treated cells, $n$=85 for rFBN1-N-treated cells, $n$=65 for rF23-treated cells; *$P$<0.5, **$P$<0.01 indicates significance compared with PC, as assessed by Student's $t$-test.